CRC Handbook of Thermal Engineering
2nd Ed., editor Raj P Chhabra, CRC Press, 2018
pp. 393-416

3.4.3 Melting and Freezing

Vasilios Alexiades
Mathematics, University of Tennessee, Knoxville, TN, USA

Jan Kosny
Fraunhofer Center for Sustainable Energy Systems, Boston, MA, USA

3.4.3 Melting and Freezing

Vasilios Alexiades and Jan Kosny

3.4.3.1 Introduction

Phase change processes, and latent heat storage, play an important role in many areas of our lives, including materials manufacturing (casting of metals and plastics, crystal growth), food preservation (freezing and thawing, freeze dehydration), medical technologies (cryosurgery, cryopreservation of tissues), transportation (aircraft icing), powerline and pipeline icing, energy conservation (latent heat storage), among many others.

Melting and freezing are among the most familiar processes in everyday life. Melting occurs when a solid is heated above its melting point T_m and changes phase from solid to liquid. At T_m the solid and liquid phases co-exist in thermodynamic equilibrium. The melting point of a pure substance depends on pressure; its value is usually specified at standard (atmospheric) pressure. Conversely, lowering the temperature of a liquid below T_m, normally results in formation of solid; the process is called freezing, solidification, or crystallization.

The primary quantities involved in describing melting/freezing are: thermal energy (enthalpy), which consists of sensible heat and latent heat, along with temperature, composition, and pressure in some cases.

In a solid, atoms are held together by strong intermolecular forces, and vibrate about stable positions. Atoms in a liquid have higher (thermal) energy, are only loosely bound, and vibrate much more. It takes a certain amount of energy, L Joules per gram, to break the bonds of a solid and render it a liquid. This energy L is called **latent heat** of melting.

Physically, a change of phase occurs due to loss of thermodynamic stability in favor of another, more favorable, phase. Below T_m, the solid configuration has lower free energy so it is more stable. At T_m, solid and liquid have the same free energy, but their enthalpies differ by L. Above T_m, liquid has lower free energy, so it is favored thermodynamically and thus a solid melts by absorbing the latent heat. The most prominent feature is the absoption or release of latent heat. The region where this occurs is the **interface**, where the phases coexist and across which the enthalpy jumps by L. Its thickness may be a few Angstroms or several centimeters, and its structure may be very complex, depending on several factors (composition, rate of cooling, temperature gradients, surface tension, supercooling, etc).

Mathematically, such problems are called **moving boundary problems** (free boundary problems when time-independent). The location of the interface, being unknown, renters such problems de facto *nonlinear*, the major source of difficulty in treating them.

The latent heat concept was introduced by Joseph Black (1728-1799) who found it experimentally in 1758-1762. Lame-Clapeyron in 1831 incorporated latent heat into heat conduction, and in the early 1860s Franz Neumann (1798-1895) found the similarity solution that bears his name (§3.4.3.2). Jozef Stefan (1835-1893) formulated clearly the Stefan problem in 1889 in studying freezing of soil, discussed in §3.4.3.2.

The melt point T_m and the latent heat L are found experimentally, commonly with Differential Scanning Calorimetry (DSC). Pure crystaline solids melt at a well-determined temperature T_m, whereas amorphous solids and mixtures or alloys typically melt over an an interval of temperatures.

3.4.3.1-A Solidification and Supercooling

Freezing, or solidification, the reverse of melting, is a phase transition process in which a liquid turns into a solid when its temperature is lowered below its freezing point. Ideally, the freezing point and heat of fusion of a melt would be the same as the melting point and latent heat of melting of the material. However, creating a stable crystaline structure is much harder than taking one apart, so the phenomenon of **supercooling** often arises, (sometimes also referred to as "undercooling"), whereas superheating is very rare.

At the **microscopic level**, crystalization proceeds by nucleation and subsequent crystal growth. The first step is *nucleation*, in which molecules start to form nano-sized clusters, arranging themselves in the lattice pattern that defines the crystal structure of the material being solidified. There is an energy barrier for (homogeneous) nucleation: if a nucleus is too small, the amount of energy bound in its volume may not be sufficient to create its surface. Thus the liquid may supercool significantly below T_m without crystalizing. However, this is a thermodynamically *metastable* state, small perturbations will induce rapid nucleation. The presence of seed crystals or foreign particles, even dust, provides sites for (heterogeneous) nucleation, reducing the degree of supercooling. Following nucleation, growth of stable nuclei is governed by free energy minimization considerations, involving competition between volume and surface terms and other effects (surface tension, curvature, capilarity, Marangoni effects, etc). The structure of the interface may be planar, columnar, dendritic, or amorphous, and difficult to model. This is a large and still active field of research in materials science, concerned with microstructural evolution and morphological instabilities, as they impact the strength of the resulting solid and various of its properties [Colin 2014], [Kim 1978], [Zaeema and Mesarovicb 2011]. In the following, we concentrate on **macroscopic aspects** and do not further discuss microstructural/morphological aspects.

Figure 3.4.13 depicts DSC measured data for n-Octadecane paraffin. A small hysteresis between melting and freezing curves can be seen, the melting point is $27°C$ and the freezing point $26°C$. Measuring the melting point T_m is more reliable and reproducible, whereas the freezing point is not considered to be a characteristic property of the material.

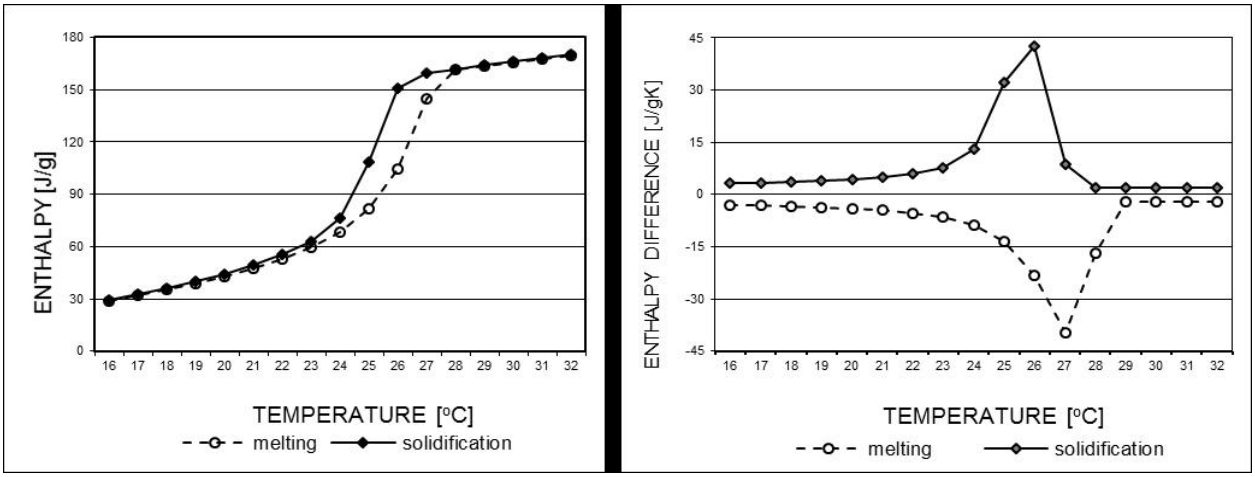

Figure 3.4.13: Differential Scanning Calorimeter (DSC) data for n-Octadecane.
Left: enthalpy vs temperature. Right: enthalpy difference curves for melting and freezing.

There are several inorganic substances (hydrated salts), called congruent, which melt and solidify cleanly, with the liquid and solid phases having the same chemical composition. In semi-congruent substances, a salt hydrate and an aqueous solution are formed during the fusion process. This reaction needs to be overturned before freezing to avoid volume reduction of the active phase changing material, which compromises the overall system thermal performance. Usually, semi-congruent melting substances can be modified with additives to render them congruent. Some combinations of an anhydrous salt and an aqueous solution can become incongruent during melting. Unless such material is modified, the anhydrous salt will settle down due to gravity, resulting in a gradual loss in heat storage performance. The most suitable methods of preventing this process are either through thickening the salt solution or through gelling. Thickening means addition of a material to the salt hydrate that increases the viscosity and hereby holds the salt hydrate together [Farid 2004], [Mehling and Cabeza 2008]. Gelling means adding a cross-linked material (e.g. polymer) to the salt to create a three dimensional network that holds the salt hydrate together, so that, when anhydrous salt crystals are formed, phase separation does not occur.

3.4.3.1-B Phase diagrams

The thermodynamic state of a material is determined by its temperature T, pressure P, and composition C. Equality of temperatures ensures thermal equilibrium, equality of pressures ensures mechanical equilibrium, and equality of chemical potentials ensures chemical equilibrium. Phases are regions in (T, P, C)-space where the material is thermodynamically stable. Phase transitions occur along boundaries between different phases. They are represented commonly by 2D phase diagrams which are projections on the (T, P)-plane or (C, T)-plane, etc.

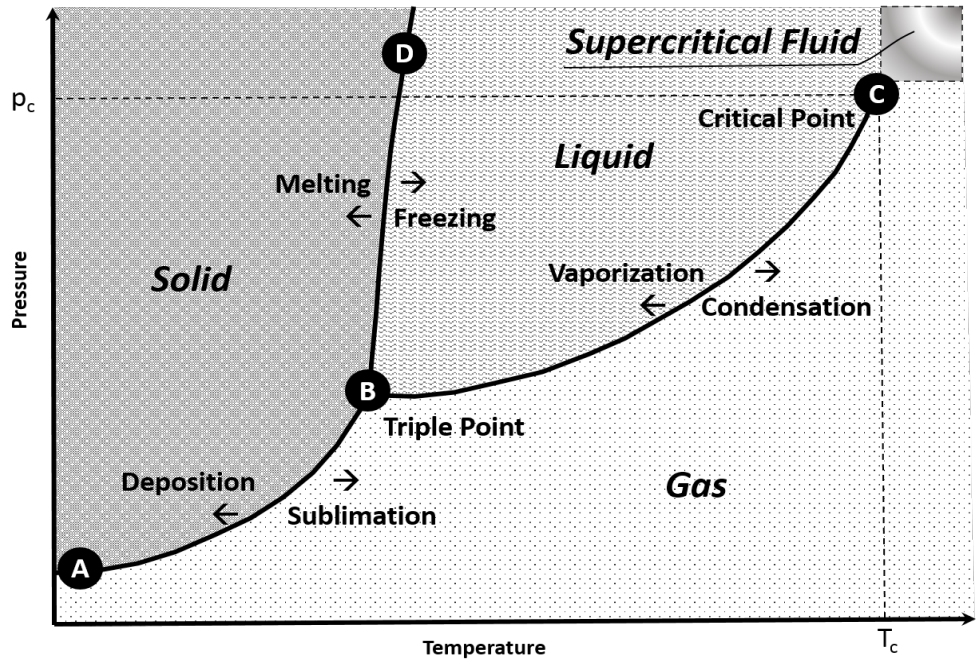

Figure 3.4.14: Schematic phase diagram showing the phases of a pure substance as function of temperature and pressure.

Figure 3.4.14 depicts a phase diagram which summarizes the effect of temperature and pressure on a pure substance in a closed container. The melting point of a substance depends on pressure and is usually specified at standard pressure. The phase diagram shown in the figure is divided into three main areas, which represent the solid, liquid, and gaseous states of the substance. The point B, called the Triple Point, represents the only combination of temperature and pressure at which a pure substance can exist simultaneously as a solid, a liquid, and a gas phase. The line between points B and D, representing solid-liquid equilibria, has, for most materials, a small positive slope. It is because melting points of most solids do not depend very much on changes in pressure. However, for water, the slope of this line is slightly negative because water can melt at temperatures near its freezing point when subjected to increased pressure. The line connecting points A and B represents solid-gas equilibria. At these temperatures and pressures, the rate at which the solid sublimes to form a gas is equal to the rate at which the gas turns into a solid. Similarly, the solid line between points B and C shows for gases and liquids the temperature dependence of the vapor pressure. Besides, in the top right corner, above the critical point, the supercritical fluid (SCF) area is shown. Critical Point C represents the end point of a phase equilibrium curve. At the critical point, phase boundaries disappear. SCF is a phase at a temperature and pressure above its critical point, where distinct liquid and gas phases do not exist, because there is no surface tension in a SCF, as there is no liquid-gas phase boundary. That is why SCF can easily effuse through solids like a gas, and dissolve materials like a liquid.

In the general case of a multi-component, multi-phase system, the number of variables, f= degrees of freedom, needed to specify the thermodynamic state is given by the **Gibbs phase rule:** $f = 2 + N_{components} - N_{phases}$, [Lupis 1983]. Thus, for a pure material, $N_{components} = 1$, so in the liquid or solid: $f = 2 + 1 - 1 = 2$, namely T and P, whereas along a phase coexistence curve: $f = 2 + 1 - 2 = 1$, so only one of T, P suffices. On the other hand, for a binary system $N_{components} = 2$, so in the liquid or solid: $f = 2 + 2 - 1 = 3$, namely T, P, C needed, whereas in the mushy region of the phase diagram $N_{phases} = 2$, so $f = 2$.

For multi-component materials (alloys, blends, mixtures), the C-T phase diagram (at a fixed pressure) can be very complex, and the effect of composition is much more dramatic than that of pressure.

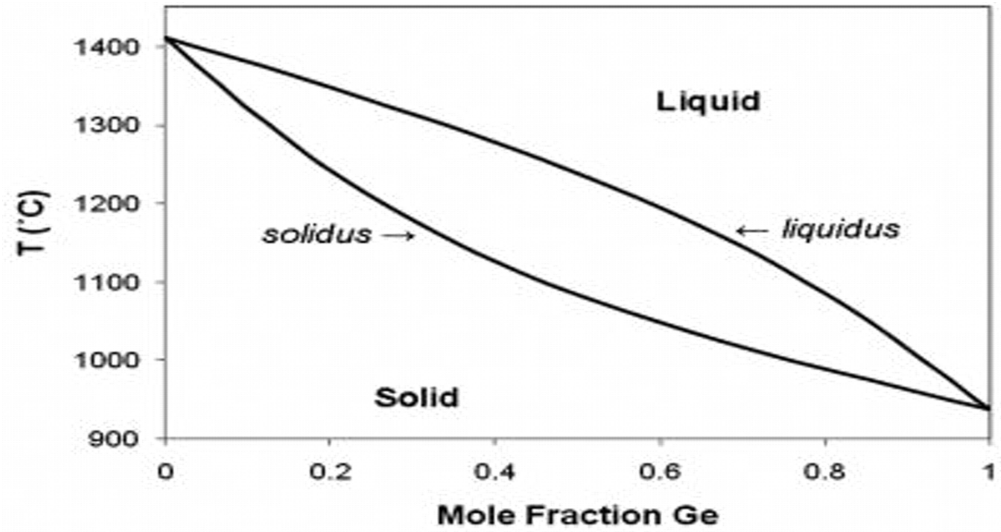

Figure 3.4.15: Phase diagram of Si-Ge binary alloy.

The simplest phase diagram for a binary alloy arises when the two components A and B are soluble in all proportions into each other, as is the case for Si-Ge shown in Figure 3.4.15. The lens-shaped region between solidus and liquidus curves is a mushy region, containing states (C, T) which are mixtures of solid and liquid of different compositions coexisting at equilibrium. This miscibility gap arises from equality of chemical potentials of coexisting phases for each component, as required for thermodynamic equilibrium, [Lupis 1983]. Cooling down liquid at some composition C_o (% fraction of component B), solidification begins at $T_o = T^{liquidus}(C_o)$. But at that temperature, liquid of composition C_o is at equilibrium with solid at composition $C^{solidus}(T_o)$, which is what will precipitate out of solution at first. This enriches B in liquid and creates segregation of components, which will set up mass diffusion in the liquid, and concurrently the released latent heat must be transfered away before the temperature can be reduced further. It is a coupled conduction-diffusion process. The solid forming will be progressively richer in B, of compositions determined by the lever rule. The mean composition remains at C_o, and the mushy material is **constitutionally supercooled**. This will continue till the temperature decreases down to $T^{solidus}(C_o)$. Thus, here solidification occurs over the extended temperature range from $T^{liquidus}(C_o)$ down to $T^{solidus}(C_o)$. A more detailed discussion can be found in [Alexiades and Solomon 1993 §2.5].

3.4.3.1-C Other effects

Many different physical phenomena *may* influence a melting process, and especially a freezing process, that can greatly complicate the situation. They include:

- heat and mass transfer by conduction/convection/radiation,
- possible gravitational, chemical, elastic, electromagnetic effects,
- variation of thermophysical properties,
- variation of phase-change temperature,
- density changes,
- latent heat evolution over an interval of temperatures (rather than at a single T_m),
- nucleation difficulties, supercooling,
- surface tension/capilarity/Marangoni, curvature effects.

This is a daunting list. The last two operate at microscopic scales and pertain only to microstructure during solidification. The rest operated at macroscopic scales for any phase change process. It is always necessary to make reasonable simplifying assumptions and focus only at essentials relevant to a specific investigation. It is better to start with basic ingredients and progressively incorporate more effects, if it is deemed necessary.

The core ingredients which give rise to the Stefan Problem (discussed in the next section) and which are widely applicable in many situations are the following:

- heat transfer by conduction only,
- pure material,
- constant thermophysical properties in each phase,

- phase-change temperature is fixed at some known T_m,
- density is constant and the same in both phases (else there will be moverment, hence convection, bringing in the Navier-Stokes equations!),
- latent heat is released or absorbed at T_m,
- microscopic aspects are ignorable.

With this in mind, in the next section we discuss the formulation and (exact) solution of the 1-dimensional Stefan Problem, which in fact serves as prototype of all phase change problems. In §3.4.3.3, some analytical approximations (quasistationary) and melt-time estimates are presented. Finally, in §3.4.3.4, numerical methods are discussed, concentrating on the enthalpy formulation, its discretization, and algorithm.

3.4.3.2 The Stefan Problem

The prototype of all phase change problems is the so-called **Stefan Problem**, named after Jozef Stefan (1835-1893), even though it had been studied by Lame-Clapeyron in 1831, and an explicit solution found by Franz Neumann (1798-1895) in 1860's.

The Stefan Problem is a mathematical model for melting a solid, or freezing a liquid, by heat conduction, assuming the phases are separated by a (locally planar) *moving* front, whose position at time t, denoted $x = X(t)$, is to be found along with the temperature field $T(x, t)$. The phase change front (interface) is assumed to be sharp, a surface, of zero thickness, along which the temperature is the melting temperature T_m and where the latent heat is absorbed or released.

As mentioned at the end of §3.4.3.1-C, the major physical simplifying assumptions are: pure material, of constant density (and same in both phases), changing phase at a known T_m, with sharp interface.

Analytical solutions for phase change processes in pure substances are discussed in [Evans 1951], [Carslaw and Jaeger 1959], [Rubinstein 1971], [Crank 1984], [Hill 1987], [Alexiades and Solomon 1993], among others. Today, the solution of the Stefan Problem is widely considered as one of the mostly used analytical solutions for one-dimensional solid-liquid phase transition.

3.4.3.2-A One-phase Stefan Problem

The simplest possible phase change problem involves melting of a phase change material (PCM) which is initially *solid at its melting temperature* T_m, by imposing a temperature $T_L > T_m$ on its surface, in one space dimension (a rod or a slab, insulated laterally).

Physical problem: *slab at T_m melting from the left*:
Consider a slab $0 \leq x \leq \ell$ of phase change material whose melting temperature is T_m and latent heat of melting L. Initially the PCM is *solid at temperature* T_m. Melting is induced by imposing a temperature $T_L > T_m$ at the left face $x = 0$ (while keeping the right face $x = \ell$ at T_m).

A melt-front $x = X(t)$ appears at $x = 0$ which advances into the solid while the liquid is getting hotter. At any $t > 0$, the region $0 \le x \le X(t)$ is liquid at temperature $T(x,t)$ and the rest remains solid at $T = T_m$. We assume constant thermophysical properties: density ρ, latent heat L, specific heat c_L, and thermal conductivity k_L (hence constant thermal diffusivity $\alpha_L = k_L/\rho c_L$).
The mathematical problem modeling this process is the following

One-phase Stefan Problem (for a slab initially at T_m melting from the left):

Find the interface location $X(t)$, $t > 0$, and the temperature $T(x,t)$, $0 \le x \le X(t)$ $t > 0$, such that:

$$T_t = \alpha_L\, T_{xx} \qquad \text{for} \quad 0 < x < X(t),\ t > 0 \quad \text{(in liquid)} \tag{3.4.40}$$

$$T(X(t),t) = T_m,\ t > 0, \qquad \text{(interface temperature} = T_m\text{)} \tag{3.4.41}$$

$$\rho L X'(t) = -k_L T_x(X(t),t) \ \ t > 0, \quad \text{(Stefan condition)} \tag{3.4.42}$$

$$X(0) = 0 \qquad \text{(initially all solid)} \tag{3.4.43}$$

$$T(0,t) = T_L > T_m, \quad t > 0 \qquad \text{(imposed temperature} = T_L\text{)} \tag{3.4.44}$$

Subscripts "t" and "x" denote partial derivative with respect to t and x, and $X'(t) = dX/dt$ in (3.4.42) is the speed of the interface. The **Stefan condition** (3.4.42), expressing conservation of energy *across* the interface, is the additional condition needed to find the additional unknown $X(t)$. It says that the latent heat absorbed at the front equals the jump of heat flux $[\![q]\!]_S^L \equiv q_L - q_S = -k_L T_x - 0$ across the front (here heat flux in solid $q_S = 0$ since $T \equiv T_m$); see (3.4.51) below.

Note that, since the solid remains at T_m, the back face $x{=}\ell$ plays no role here, so the slab may be considered as extending to infinity. The problem admits a (similarity) solution, known as **Neumann solution**, provided all parameters and data are constants [Alexiades and Solomon 1993, p.35]. It is expressed in terms of a single parameter λ which is the root of (3.4.47) below.

Interface location:

$$X(t) = 2\,\lambda\sqrt{\alpha_L\, t}, \quad t > 0 \tag{3.4.45}$$

Temperature in liquid region $0 < x < X(t)$, $t > 0$:

$$T(x,t) = T_L - (T_L - T_m)\frac{\operatorname{erf}\left(\frac{x}{2\sqrt{\alpha_L\, t}}\right)}{\operatorname{erf}(\lambda)}. \tag{3.4.46}$$

The parameter λ is the unique solution to the transcendental equation

$$\lambda\, e^{\lambda^2} \operatorname{erf}(\lambda) = \frac{St_L}{\sqrt{\pi}}\,, \qquad \text{where} \quad St_L = \frac{c_L(T_L - T_m)}{L} = \text{Stefan Number}\,, \tag{3.4.47}$$

with erf() the error function.

For each $St_L > 0$, the transcendental equation (3.4.47) has unique solution $\lambda > 0$ which depends only on the (dimensionless) parameter St_L. It can be computed easily by any root finder, e.g. bisection or Newton-Raphson.

The **Stefan Number** St is the ratio of *sensible heat* $c\,\Delta T$ to *latent heat* L, and it completely characterizes the 1-phase Stefan problem (as can be seen by undimensionalization, [Alexiades

and Solomon 1993, p.37]. Small St signifies that latent heat dominates, whereas large St indicates that sensible heat dominates. Water and certain waxes have high latent heat, while metals have low latent heat. In particular, water has very high $L = 333.4$ J/g, so it is an excellent heat storage material. For example, in melting of ice at $T_m = 0°$C by holding it at body temperature $T_L = 37°$C we have $St_L = 0.46$ (for water $c_L = 4.2$ J/g·K). Similarly, in food freezing from $T_m = 0$ to $T_S = -20°$C, $c_S \approx 2$ J/gK and so $St_S = c_S(T_m - T_S)/L = 0.12$.

The Neumann solution (3.4.45)-(3.4.47) is in fact the *unique* solution of the 1-phase Stefan Problem. It shows that the front location is proportional to the square root of time, so it starts with infinite speed at $t = 0$ (to accomodate the initial discontinuity at $x = 0$). Solving (3.4.45) for t gives the time for the melt front to reach a specific location x=x_o: $t_{melt}(x_o) = x_o^2/(4\lambda^2\alpha_L)$.

For small $S_L \approx 0$, the root λ is also small and to first order $\lambda \approx \sqrt{(St_L/2)}$. This provides a good starting value for Newton-Raphson iteration. Then also the ratio of erf()'s in (3.4.46) is $\approx x/X(t)$, so the Neumann temperature becomes $T(x,t) \approx T_L - (T_L - T_m)x/X(t)$. Thus at each time t the temperature is a line joining the point (x=0, T=T_L) with (x=$X(t)$, T=T_m).

The analogous **freezing** problem, and its solution, can be obtained by simply replacing the subsrcipt "L" by "S" and the latent heat L by $-L$. In this case the imposed temperature will be $T_S < T_m$ and the Stefan number for solid will be $St_S = (T_m - T_S)/L$.

3.4.3.2-B Two-phase Stefan Problem

A more realistic case is melting of a solid initially colder than T_m. Then there will be heat transfer in both phases.

Physical problem: *slab melting from the left*:
Consider a slab $0 \le x \le \ell$ of phase change material whose melting temperature is T_m and latent heat of melting is L. Initially the material is solid at some temperature $T_S < T_m$. Melting is induced by imposing an elevated temperature $T_L > T_m$ at the left face ($x = 0$), while keeping the right face ($x = \ell$) insulated. We assume constant thermophysical properties: density ρ, latent heat L, specific heats c_L, c_S, thermal conductivities k_L, k_S (hence constant thermal diffusivities $\alpha_L = k_L/\rho c_L$ and $\alpha_S = k_S/\rho c_S$, and a sharp interface $x = X(t)$.

At each time t, liquid occupies $[0, X(t))$ and solid $(X(t), \ell]$, separated by the melt front $x = X(t)$. Conservation of (thermal) energy *in each phase* is expressed by the heat conduction equation for temperature $T(x,t)$, and the Stefan condition expresses conservation of energy *across* the interface. The mathematical problem modeling this process is the following

Two-phase Stefan Problem (for a slab melting from the left):

> Find the temperature $T(x,t)$, $0 \le x \le \ell$, $t > 0$, and interface location $X(t)$, $t > 0$, such that:

$$T_t = \alpha_L\, T_{xx} \qquad \text{for } 0 < x < X(t),\ t > 0 \quad \text{(in liquid)} \tag{3.4.48}$$

$$T_t = \alpha_S\, T_{xx} \qquad \text{for } X(t) < x < \ell,\ t > 0 \quad \text{(in solid)} \tag{3.4.49}$$

$$T(X(t), t) = T_m,\ t > 0, \qquad \text{(interface temperature} = T_m) \tag{3.4.50}$$

$$\rho L X'(t) = -k_L T_x(X(t), t) + k_S T_x(X(t), t), \quad t > 0, \quad \text{(Stefan condition)} \tag{3.4.51}$$

$$X(0) = 0 \qquad \text{(initially all solid)} \tag{3.4.52}$$

$$T(x, 0) = T_S < T_m, \quad 0 \le x \le \ell \qquad \text{(initial temperature} = T_S) \tag{3.4.53}$$

$$T(0, t) = T_L > T_m, \quad t > 0 \qquad \text{(imposed temperature} = T_L) \tag{3.4.54}$$

$$-k_S T_x(\ell, t) = 0, \qquad t > 0 \qquad \text{(insulated boundary)} \tag{3.4.55}$$

The problem (3.4.48)-(3.4.56) stated above does *not* admit an exact analytical solution. However, considering it on the semi-infinite slab $[0, \infty)$ (with the boundary condition (3.4.55) replaced by $\lim_{x->\infty} T(x, t) = T_S$), the problem *does* admit a (similarity) solution, provided all parameters and data are constants, [Alexiades and Solomon 1993, p.47].

Neumann solution of the 2-phase Stefan Problem:
Interface location:

$$X(t) = 2\,\lambda\sqrt{\alpha_L\, t}, \quad t > 0 \tag{3.4.56}$$

Temperature in liquid region $0 < x < X(t),\ t > 0$:

$$T(x, t) = T_L - (T_L - T_m)\frac{\operatorname{erf}\left(\frac{x}{2\sqrt{\alpha_L\, t}}\right)}{\operatorname{erf}(\lambda)}, \tag{3.4.57}$$

Temperature in solid region $x > X(t),\ t > 0$:

$$T(x, t) = T_S + (T_m - T_S)\frac{\operatorname{erf}\left(\frac{x}{2\sqrt{\alpha_S\, t}}\right)}{\operatorname{erfc}\left(\lambda\sqrt{\alpha_L/\alpha_S}\right)}. \tag{3.4.58}$$

The parameter λ is the solution to the transcendental equation

$$\frac{St_L}{\exp(\lambda^2)\,\operatorname{erf}(\lambda)} - \frac{St_S}{\nu\exp(\nu^2\,\lambda^2)\,\operatorname{erfc}(\nu\,\lambda)} = \lambda\,\sqrt{\pi}\,, \tag{3.4.59}$$

where

$$St_L = \frac{c_L(T_L - T_m)}{L}\,, \quad St_S = \frac{c_S(T_m - T_S)}{L}\,, \quad \nu = \sqrt{\frac{\alpha_L}{\alpha_S}}\,, \tag{3.4.60}$$

and erfc()=1−erf() the complimentary error function.

Note that the value of λ depends only on the two **Stefan numbers** St_L, St_S, and the diffusivity ratio ν. The (dimensionless) transcendental equation (3.4.59) has exactly one root λ for each $St_L > 0$, $St_S \ge 0$, $\nu > 0$ [Alexiades and Solomon 1993, p.48)], which can easily be found using a root finder.

Small $St_L \approx 0$ implies small λ, and then to first order (3.4.59) is approximately $St_L/(2\lambda^2) - St_S/(\nu\lambda\sqrt{\pi}) = 1$, whence

$$\lambda \approx \frac{1}{2}\left[-\frac{St_S}{\nu\sqrt{\pi}} + \sqrt{2St_L + \left(\frac{St_S}{\nu\sqrt{\pi}}\right)^2}\right] \quad \text{for } St_L \approx 0. \tag{3.4.61}$$

If, in addition, $St_S \gg St_L \approx 0$, this simplifies to $\lambda \approx (\nu\sqrt{\pi}/2)\,(St_L/St_S)$.

Setting $T_S = T_m$, whence $St_S = 0$, the 2-phase Neumann solution reduces to the 1-phase solution.

The analogous **freezing** problem, and its solution, is obtained by simply exchanging the subsrcipts "L" and "S" and replacing the latent heat L by $-L$.

3.4.3.3 Analytical Approximations

Exact explicit solutions, presented in §3.4.3.2, provide complete information on how parameters influence the solution and what one to expect, but exist only for the simplest Stefan Problem, only in semi-infinite problems, and only for parameters constant in each phase. Moreover, very few explicit solutions are known in cylindrical or spherical geometries, and none for finite domains and higher dimensions.Thus for most realistic problems one must seek approximate solutions, of which there are two classes: *analytical approximations*, discussed in this section, and *numerical approximations*, discussed in the next section.

The four main types of analytical approximations for phase change problems in use are known as the *quasistationary approximation*, the *Megerlin method*, the *heat balance integral*, and the broad class of *perturbation expansions*. The last one is a general classical methodology of applied mathematics, that seeks solutions in the form of a series expansion in some small parameter entering the problem.

The applicability of the other methods relies on being able to simplify the problem to a form that fits the method, which then can generate solvable problems. The resulting solution may turn out to be quite accurate, at least for standard, simple processes. However, there is no way of checking the validity of physical simplifications made, and there are no a priori error estimates for the mathematical approximations. The validity of an analytical approximation may be judged only by comparing with some other independently validated method and only for a class of very similar problems. Thus, at best they can provide only qualitative "order of magnitude" information rather than quantitative results, and they are limited to only for 1-phase in one dimension. Nevertheless, when they work, they are very useful for rough sizing estimates of melt depth, melt time, heat flux, etc.

It should be noted that nowadays, in view of the versatility and relative easy of applying direct computational methods, only simple, easy to apply and easy to evaluate analytical solutions are really useful. And in fact, being analytic expressions, they can reveal qualitative behavior, e.g. dependence on parameters, in ways that numerical calculations cannot.

A word of warning on terminology: sometimes in the literature analytical approximations are advertised as "exact solutions" because an approximate problem is solved "exactly".

Below we present only the basics of the quasistationary approximation and some useful melt-time estimates, referring for more details and other methods to [Ozisik 1993], [Alexiades and Solomon 1993, ch.3] for details.

The quasistationary (or quasistatic) approximation is the simplest of the analytical approximation, well suited for "back of the envelope" sizing estimates. It can be applied only to 1-phase Stefan problem, but for any of the standard boundary conditions at $x = 0$.

It is based on the physical assumption that *the sensible heat in the process is negligible compared to the latent heat*. This amounts to assuming small Stefan Number: $St \approx 0$

The quasistationary approximation consists of replacing the heat equation by the steady-state equation $T_{xx} = 0$, while the front still varies in time. Thus $T(x,t)$ is linear in x, and the temperature profile at any time can be found using the boundary conditions. Then the front location is found from the Stefan condition. We present the approximations for the standard boundary conditions below.

3.4.3.3-A Quasistationary approximation for imposed temperature

The quasistationary approximation of the 1-phase Stefan Problem with imposed temperature at $x = 0$, which may be varying in time: $T(0,t) = T_L(t)$, is the following [Alexiades and Solomon 1993, p.128]:

$$X^{qs}(t) = \left(2\frac{k_L}{\rho L}\int_0^t [T_L(s) - T_m]ds\right)^{1/2}, \quad t \geq 0, \tag{3.4.62}$$

$$T^{qs}(x,t) = T_L(t) - [T_L(t) - T_m]\frac{x}{X^{qs}(t)}, \quad 0 \leq x \leq X^{qs}(t),\ t \geq 0, \tag{3.4.63}$$

When $T_L(t) \equiv T_L = const.$ this simplifies to

$$X^{qs}(t) = 2\sqrt{St_L/2}\,\sqrt{\alpha_L\, t}\,, \quad t \geq 0, \tag{3.4.64}$$

$$T^{qs}(x,t) = T_L(t) - [T_L(t) - T_m]\frac{\frac{x}{2\sqrt{\alpha_L\, t}}}{2\sqrt{St_L/2}}, \quad 0 \leq x \leq X^{qs}(t),\ t \geq 0. \tag{3.4.65}$$

which is in fact the Neumann solution for the case $St_L \approx 0$. If follows that the quasistationary front $X^{qs}(t)$ *overestimates* the actual front $X(t)$ and also $T^{qs}(x,t) > T(x,t)$.

3.4.3.3-B Quasistationary approximation for imposed flux

For imposed flux boundary condition at $x = 0$, namely, $-k_L\frac{\partial T}{\partial x}(0,t) = q_L(t) > 0$, for a given $q_L(t)$, there is no explicit solution available, even for constant q_L. The quasistationary solution is easily found to be [Alexiades and Solomon 1993, p.134–136]

$$X^{qs}(t) = \frac{1}{\rho L}\int_0^t q_L(s)ds, \quad t \geq 0 \tag{3.4.66}$$

$$T^{qs}(x,t) = T_m + \frac{q_L(t)}{k_L}\left[X^{qs}(t) - x\right], \quad 0 \leq x \leq X^{qs}(t),\ t \geq 0 \tag{3.4.67}$$

Example: *constant flux* $q_L(t) \equiv q_L$. For constant imposed flux, the quasistationary temperature is linear in both x and t, the face temperature $T^{qs}(0,t)$ grows linearly in time, and the melt-time of a location x is $t^{qs}_{melt}(x) = \rho\, L\, x/\, q_L$.

Example: *sinusoidal flux* $q_L(t) = q_{max}\, sin(\frac{\pi t}{2t_o})$. The solution is easily found, and

one can check that at after a full cycle $2t_o$,

$$X^{qs}(2t_o) = \frac{4\,t_o\,q_{max}}{\rho L\,\pi}, \quad T^{qs}(x, 2t_o) = T_m \ \text{ (but liquid).} \tag{3.4.68}$$

3.4.3.3-C Quasistationary approximation for convective boundary condition

The boundary condition for convective heating at $x = 0$ by an ambient temperature $T_L(t) > T_m$, with heat transfer coefficient h, is

$$-k_L \frac{\partial T}{\partial x}(0,t) = h\,[T_L(t) - T(0,t)], \quad t > 0. \tag{3.4.69}$$

The quasistationary solution of the Stefan Problem turns out to be [Alexiades and Solomon 1993, p.137–139]

$$X^{qs}(t) = \frac{-k_L}{h} + \left(\frac{k_L^2}{h^2} + 2\,\frac{k_L}{\rho L}\int_0^t [T_L(s) - T_m]ds\right)^{1/2}, \quad t \geq 0 \tag{3.4.70}$$

$$T^{qs}(x,t) = T_m + [T_L(t) - T_m]\,\frac{h\,[X^{qs}(t) - x]}{h\,X^{qs}(t) + k_L}, \quad 0 \leq x \leq X^{qs}(t),\ t \geq 0 \tag{3.4.71}$$

and the temperature and flux at the face $x = 0$ are

$$T^{qs}_{face}(t) = \frac{T_m + \frac{h\,X^{qs}(t)}{k_L}\,T_L(t)}{1 + \frac{h\,X^{qs}(t)}{k_L}}, \quad t \geq 0, \tag{3.4.72}$$

$$q^{qs}_{face}(t) = \frac{k_L}{X^{qs}(t)}\,[T^{qs}_{face}(t) - T_m], \quad t \geq 0. \tag{3.4.73}$$

Solutions for axially or radially symmetric processes can be found in [Alexiades and Solomon 1993, pp.144–152].

3.4.3.3-D Melt-time for a simple PCM body with imposed temperature

Consider a PCM initially solid at T_m, being melted due to a high temperature $T_L > T_m$ imposed on its boundary. Assume the melting process can be described in terms of a single *effective length* r, $0 \leq r \leq \ell$. If A is the surface area across which heat is transfered into the PCM and V its volume, define the **shape factor** ω by

$$1 + \omega = \ell\,A/V\,. \tag{3.4.74}$$

Then $\omega = 0$ for a PCM slab or rod of length ℓ insulated at one end, $\omega = 1$ for a PCM cylinder of radius ℓ heated radially, and $\omega = 2$ for a PCM sphere of radius ℓ. Note that $0 \leq \omega \leq 2$ always.

The 1-phase (inward) melting process, for any $0 \le \omega \le 2$, may be formulated as follows:

$$\frac{\partial T}{\partial t} = \frac{\alpha_L}{r^\omega}\frac{\partial}{\partial r}\left(r^\omega \frac{\partial T}{\partial r}\right), \qquad R(t) \le r \le \ell, \quad t > 0, \tag{3.4.75}$$

$$T(R(t),t) = T_m\,, \qquad \rho L\, = -k_L\,(R(t),t), \quad t > 0 \tag{3.4.76}$$

$$R(0) = \ell, \qquad T(\ell,t) = T_L, \quad t > 0. \tag{3.4.77}$$

The PCM melts completely when the melt front $R(t)$ reaches $r = 0$. Letting

$$\Delta T_L = T_L - T_m \quad \text{and} \quad St_L = c_L\,\Delta T_L/L, \tag{3.4.78}$$

the melt-time of the PCM may be approximated by [Alexiades and Solomon 1993, p.169]

$$t_{melt} \approx \frac{\ell^2}{2\alpha_L(1+\omega)St_L}\left[1 + \left(0.25 + 0.17\omega^{0.7}\right)St_L\right], \text{ valid for } 0 \le St_L \le 4, \tag{3.4.79}$$

and the *average* heat flux at $r = \ell$ during the entire melting process by

$$\bar{q} \approx \frac{-2k_L\Delta T_L}{\ell}\left[1 + (0.121 + 0.0424\,\omega)St_L^{0.7645-0.2022\,\omega}\right]. \tag{3.4.80}$$

The **freezing time** of the analogous process is obtained by replacing the subscript $_L$ by $_S$ and the latent heat L by $-L$.

Note that these expressions, easily computable on a calculator or spreadsheet, allow one to estimate correlations among parameters. Also note that melt-depth can be found by solving (3.4.79) for ℓ.

3.4.3.3-E Melt-time for a simple PCM body with convective boundary condition

For convective heating with heat transfer coefficient h and ambient temperature T_L, the boundary condition in (3.4.77) reads

$$-k_L\frac{\partial T}{\partial x} = h[T_L - T(\ell,t)], \quad t > 0, \tag{3.4.81}$$

and the melt-time estimate (3.4.79) becomes

$$t_{melt} \approx \frac{\ell^2}{2\alpha_L(1+\omega)St_L}\left[1 + \frac{2}{Bi} + \left(0.25 + 0.17\,\omega^{0.7}\right)St_L\right], \tag{3.4.82}$$

valid for $0 \le St_L \le 4,\ Bi \ge 0.1$, where $Bi = h\ell/k_L$ is the Biot Number of the process.

A very useful aspect of these melt-time estimates is to explore the influence of parameters, especially of the shape and size of the PCM, by varying ω and ℓ.

3.4.3.4 Numerical approaches

The literature on numerical methods for phase-change problems is a huge. Currently, a Google search produces 864,000 results!

Phase change processes are quite complex due to the presence of a moving boundary, or region, in which heat and mass balance conditions have to be met, which renters the problem non-linear, and, in addition, the simulated material often has different thermophysical characteristics in different phases [Lamberg et al. 2004].

Numerical methods for addressing phase transition problems have been reviewed in many publications, including: [Basu and Date 1988], [Idelsohn et al. 1994], [Hu and Argyropoulos 1996], [Voller et al.2006], [Dutil et al. 2011], [AL-Saadi and Zhai 2013]. The earliest computational techniques for solving phase transition problems are an enthalpy-type method [Dusinberre 1945], and a Heat Source Method [Eyres et al. 1946].

Presently used direct numerical simulations methods of phase transition processes can be classified into two categories. The first category, often referred to as **front tracking or multi-domain methods**, uses independent conservation equations in each phase region and couples them with appropriate interface conditions at the (isothermal) moving front. The second category, known as **front capturing or fixed-domain methods**, uses a single region (continuum) formulation in which the interface does not appear explicitly, but can be "captured" from the solution. Over the years, various hybrid methods have also been developed that attempt to combine aspects of both categories in order to take advantage of the best features of each methodology.

3.4.3.4-A Front Tracking Methods

Front tracking methods, also called interface tracing, apply to problems which (are assumed to) have a sharp interface whose precise location is considered crucial and should be tracked. This situation arises in pure materials without internal heating (classical Stefan problem), and in (microscopic) studies of morphological instabilities, among others.

Front tracking techniques follow the dynamic evolution of a moving interface across which physical variables are discontinuous. Usually they employ finite difference or finite volume discretization of the heat equation and the numerically defined interface is propagated by a set of topologically connected marker points so as to satisfy an explicitly imposed interface (Stefan) condition. However, it is difficult to handle topological changes such as merging fronts or appearing and disappearing phases.

Various types of tracking methods have been developed over the years, such as:
(a) fixed grid [Lazaridis 1969], [Rao and Sastri 1984];
(b) variable time step [(Douglas and Gallie 1955];
(c) variable space grid [Murray and Landis 1959];
(d) front-fixing by coordinate transformations [Crank and Gupta 1975], [Hsiao 1985];
(e) boundary integral formulations [Chuang and Szekely 1972], [ONeill 1983];
(f) Lagrangian-type adaptive meshes [Bonnerot and Janet 1977], [Lynch 1982], [Albert and ONeill 1986], [Zabaras and Ruan 1990];
(g) front tracking for shocks and flames [Glimm et al. 1998]
(h) Shyy's ELAFINT (Eulerian-Lagrangian Algorithm for INterface Tracking [Shyy et al. 1996].

It should be noted that front tracking faces several limitations which complicate the solution

procedure and restrict its applicability. These include: (a) The very formulation of the problem *assumes a priori* that there is a sharp front to be tracked, which may or may not be the case physically. (b) When the interface forms a singularity or changes its topology, tracking becomes difficult to continue beyond the singularity time. (c) It is computationally demanding, limited to modest deformation, especially when interface motion also includes expansion and contraction. The effort for significant topological changes in Lagrangian schemes seems to have reached its limit. To overcome such limitations, alternative methods arose from front-capturing techniques, including *immerded boundary* [Uverdi and Tryggvason 1992], and *level-set type methods*, discussed in the next section.

3.4.3.4-B Front Capturing Methods

In contrast to front-tracking, front-capturing methods solve the conservation law(s) over the entire region (posed in a weak-sense mathematically), irrespectively of phase, and the inteface does not appear explicitly in the formulation. Its location can be "captured" from the solution in various ways. Field variables and parameters may change discontinuously between phases, and interfaces may be either sharp or entire (mushy) regions. In this approach, general hydrodynamics (Navier-Stokes + energy balance equations) can be solved on a *fixed Eulerian grid* rather efficiently by treating both phases as a single fluid.
Front-capturing numerical approaches fall into two main classes:

I. **Volume-of-Fluid (VoF) type methods**, primarily the **enthalpy method** (presented in detail in §3.4.3.4-C). They arose from, and are very similar to, shock capturing schemes in Computational Fluid Dynamics. The interface does not appear explicitly in the formulation, so no particular structure is assumed about it a priori. It may be a sharp front or a mushy region of any extend. The volume fraction of liquid (or solid), found from conservation laws and appropriate equations of state, is used as phase indicator, to capture the location and extend of phases at each time-step. The formulations are general and applicable to complex multiphysics problems, such as multiphase flows, bubble flows, etc.

II. **Level-set and Phase-field methods** [Sethian 1999], [Sussman et al.1998], [Osher 2002]. They are concerned with precise evolution and structure of interfaces, so they are appropriate in microscopic settings when the evolution of the front needs to be followed. They can handle topological changes easily, on fixed Eulerian grids. The interface is represented as the (zero) level set of a smooth auxiliary function $\phi(x,t)$, so it is possible to compute the normal direction: $\vec{n} = \frac{\nabla\phi}{|\nabla\phi|}$, normal velocity: $\vec{v} = \frac{d\vec{x}}{dt}\cdot\vec{n}$, and mean curvature $\kappa = \nabla\cdot\vec{n}$ from ϕ. Thus, surface tension and curvature effects can be represented in detail.

The phase-field and level-set methods differ primarily in the interpretation and determination of the phase function ϕ.
In the *level-set method*, ϕ is usually taken as distance from the front and it is updated from a kinematic advection equation (but then needs to be re-intialized, which is costly).
In the *phase-field approach*, which arose from material science (Cahn-Hilliard) considerations, the function ϕ is an order parameter, normalized to be $= \pm 1$ in the bulk phases away from the front. The front is "diffuse": $-1 < \phi < 1$, and its width is controlled by a parameter in the model. The phase-field ϕ can be chosen in various ways, usually as solution of a Cahn-Hilliard-type equation, namely, an Euler-Lagrange equation for extrema of a (configurational) free energy $J(\phi)$ containing surface and volume terms, and into which various desirable physical effects can be incorporated. Many variants and improvements exist to overcome various issues. Notable are "sharp interface" versions, where ϕ is chosen

e.g. as a hyperbolic tangent of the normal vector $\vec{n}$, [Sun and Beckermann 2007]. For a review see [Qin and Bhadeshia 2010]. A comparison of some moving grid, level set, and phase field methods for the Stefan problem is reported in [Javierre et al. 2006].

3.4.3.4-C The Enthalpy Method

The so called *enthalpy* method is the simplest and most physical, versatile, adaptable, and robust numerical method available for phase-change problems in 1, 2, or 3 space dimensions [Alexiades and Solomon 1993, Chap.4]. It is the basis on which most front-capturing and many front tracking schemes are based. It is similar to Volume-of-Fluid (VoF) and shock-capturing schemes in Computational Fluid Dynamics. It is based directly on the energy conservation law

$$\frac{\partial E}{\partial t} + \nabla \cdot Q = S\,, \tag{3.4.83}$$

with $E = \rho e$ the thermal energy (enthalpy per unit volume), Q the (heat) flux, and S any internal (volumetric) energy source or sink. For heat conduction, Q is given by Fourier's law

$$Q = -k\,\nabla T \tag{3.4.84}$$

with T the temperature, and k the thermal conductivity, which may be different in different phases, and may also depend on T. The enthalpy formulation is based on two important facts:

- The Stefan condition is a "natural" interface condition: it is automatically satisfied by a (weak) solution of the energy conservation law (3.4.83) along any surface (or region) across which E experiences a jump.
- The recognition that temperature is a poor descriptor of phase, it only captures *sensible heat* but not latent heat, it stays at T_m during absorption or release of latent heat. The natural and best descriptor is (thermal) energy itself.

By solving the PDE (3.4.83) **throughout the region** (irrespectively of phase), the energy is being updated, and then we need to find the phase and the temperature T, using the appropriate *Equation of State* (EoS) relating energy and temperature. The location of the (moving) phase-change front does **not** appear explicitly in the formulation; it is found (captured) from the solution as the region where the energy jumps by an amount equal to the latent heat. It may be a sharp surface or a region, no a priori assumption about its structure is made. This is the major advantage of the enthalpy formulation over front tracking methods.

The difference between heat transfer without and with phase-change is that in the latter case the energy jumps by L (= latent heat) at T_m, whereas it is continuous in the former case. In heat conduction, the EoS is $de/dT = c_p$ = specific heat, or, per unit volume $dE/dT = C_p := \rho c_p$, i.e. $E(T)$ = integral of the volumetric heat capacity $C_p(T)$. But during a change of phase, the latent heat is evolved at $T = T_m$ and the energy jumps by ρL at T_m. The EoS now is (referring energy to *solid* at T_m):

$$E(T) = \begin{cases} \int_{T_m}^{T} C_p^S(\tau)d\tau \approx \quad C_p^S\,[T - T_m], & T < T_m \quad \text{(solid)}\ , \\ \qquad [0, \rho L], & T = T_m \quad \text{(interface)}, \\ \rho L + \ \int_{T_m}^{T} C_p^L(\tau)d\tau \approx \rho L + C_p^L\,[T - T_m], & T > T_m \quad \text{(liquid)}\ . \end{cases} \tag{3.4.85}$$

In the region where $0 \le E \le \rho L$, the phases co-exist; it is where the latent is absorbed or released. This is the "interface", which is not necessarily a sharp surface, it may be a region, often called **mushy region**.

Note that, since C_p^S and C_p^L are strictly positive, $E(T)$ depends monotonically on T, so it is invertible, i.e. can be solved for T in terms of E.
The **liquid fraction** $\lambda = 0$ in solid, $\lambda = E/\rho L$ in mushy, $\lambda = 1$ in liquid is often used as a convenient phase indicator. Thus, we have the following characterizations of phases:

$$\begin{array}{lcccccl} \text{solid} & \Leftrightarrow & E < 0 & \Leftrightarrow & \lambda = 0 & \Leftrightarrow & T < T_m\,, \\ \text{mushy} & \Leftrightarrow & 0 \le E \le \rho L & \Leftrightarrow & \lambda = E/\rho L & \Leftrightarrow & T = T_m\,, \\ \text{liquid} & \Leftrightarrow & \rho L < E & \Leftrightarrow & \lambda = 1 & \Leftrightarrow & T > T_m\,. \end{array} \tag{3.4.86}$$

Once E is updated from the energy equation, the phase can be found from (3.4.86), and then T can be found from (3.4.85).

Remark 1: The case of *non-isothermal* phase change, occuring over an extended temperature range $[T^{solidus}, T^{liquidus}]$ may be accomodated by replacing $T = T_m$ in the above by $T^{solidus} \le T \le T^{liquidus}$.
In fact, instead of the simple EoS (3.4.85) more general equations of state may be used, see [Alexiades and Autrique 2010].

Remark 2: We emphasize again that the front is **not** being tracked, it does not even appear explicitly in the formulation. It can be *captured* from the solution as the region where $0 \le E \le \rho L$, see (3.4.108).

Remark 3: The meaning of (3.4.83), when E and Q are discontinuous, needs to be clarified. In fact, it must be interpreted in a *weak* sense mathematically, see [Alexiades and Solomon 1993, Chap.4].

3.4.3.4-D Enthalpy scheme

The energy conservation law (3.4.83) is valid in any number of (space) dimensions, for any appropriate constitutive law for flux Q, interpreted in weak sense mathematically. It may be discretized by Finite Differences or Finite Volumes or Finite Elements. The Finite Volume discretization is the most physical, and easiest to implement computationally, so we present below an algorithm for the **Finite Volume enthalpy scheme**, for a typical heat transfer problem, in one space dimension for simplicity. It can be extended to 2 of 3 dimensions easily.

To be specific, consider heat transfer in a slab occupying the region $\Omega = [a, b]$, initially at temperature $T = T_{init}(x)$, with convective heating at the left wall $x = a$, with heat transfer coefficient h and ambient $T_{amb}(t) \ge T_m$, while keeping the back end $x = b$ insulated. If $T_{init}(x) \le T_m$ and $T_{amb}(t) \ge T_m$ then this would be a 2-phase Stefan Problem, more general than in §3.4.3.2-B. The material parameters involved are: $\rho = \text{const.}$, c_p^L, c_p^S, k_L, k_S, h (which may depend on T), along with T_m and L.

The enthalpy formulation of the above problem is as follows:

$$\begin{aligned}
\text{energy conservation} \quad & E_t + Q_x = 0, \quad a < x < b,\ 0 < t \le t_{end}, && (3.4.87)\\
\text{constitutive law:} \quad & Q = -k\,T_x\,, && (3.4.88)\\
\text{equation of statei} \quad & (3.4.85) &&\\
\text{initial condition:} \quad & T(x,0) = T_{init}(x),\ a \le x \le b, && (3.4.89)\\
\text{boundary conditions:} \quad & Q(a,t) = h\,[T_{amb}(t) - T(a,t)], \quad Q(b,t) = 0 \quad t > 0, && (3.4.90)
\end{aligned}$$

for given $T_{init}(x)$ and $T_{amb}(t)$. The only difference with plain heat conduction is the jump of energy in the EoS (3.4.85), which encodes the latent heat effect.

Space mesh: Choose an integer M and partition the interval $\Omega = [a,b]$ into M control volumes $V_i = [x_{i-1/2}, x_{i+1/2}]$, $i = 1, 2, \ldots, M$, of width $\Delta x_i = x_{i+1/2} - x_{i-1/2}$. Place a node point x_i in V_i, and define the array of nodes $x_0 = a$, $x_1, x_2, \ldots, x_M$, $x_{M+1} = b$. For a *uniform mesh*, $\Delta x = (b-a)/M$, and the nodes array is: $x_0 = a$, $x_1 = \Delta x/2$, $x_i = x_1 + (i-1)\Delta x$ for $i = 2, ..., M$, $x_{M+1} = b$. Note that x_0 and x_{M+1} are the boundaries, included into the mesh-array for convenience.

Time steps: Choose time-steps $\Delta t_n > 0$, small enough for accuracy and stability (see below), and define the discrete times $t_0 = 0$, $t_{n+1} = t_n + \Delta t_n$, $n = 0, 1, ...$ If $\Delta t_n = \Delta t$ for all n, then $t_n = n\,\Delta t$, and the number of time-steps to get to desired time t_{end} will be $N = t_{end}/\Delta t$.

Finite Volume discretization of (3.4.87): Integrating (3.4.87) over the i-th control volume $V_i = [x_{i-1/2}, x_{i+1/2}]$, $i = 1, ..., M$ and over the time interval $[t_n, t_n + \Delta t_n]$ gives

$$\int_{t_n}^{t_{n+1}} \frac{\partial}{\partial t} \left(\int_{x_{i-1/2}}^{x_{i+1/2}} E(x,t)dx \right) dt + \int_{t_n}^{t_{n+1}} \int_{x_{i-1/2}}^{x_{i+1/2}} \frac{\partial}{\partial x} Q(x,t)dxdt = 0, \tag{3.4.91}$$

and carrying out integration of the derivatives leads to

$$\int_{x_{i-1/2}}^{x_{i+1/2}} E(x,t)dx \,\Big|_{t_n}^{t_{n+1}} + \int_{t_n}^{t_{n+1}} [Q(x_{i+1/2},t) - Q(x_{i-1/2},t)]dt = 0, \tag{3.4.92}$$

which expresses *exact discrete conservation*. Now define the discrete mean energy and mean flux as

$$E_i^n = \frac{1}{\Delta x} \int_{x_{i-1/2}}^{x_{i+1/2}} E(x,t_n)\,dx = \text{ mean value of } E \text{ over } V_i \text{ at } t_n\ ,\ i = 1, \ldots, M, \tag{3.4.93}$$

$$\begin{aligned}
Q_{i-1/2}^{n+\theta} = \frac{1}{\Delta t} \int_{t_n}^{t_{n+1}} Q(x_{i-1/2},t)dt = & \text{ mean flux during } [t_n, t_{n+1}] \text{ through face} \\
& \text{at } x_{i-1/2}\ \text{, i=1,...,M+1,}
\end{aligned} \tag{3.4.94}$$

with *implicitness parameter* $0 \le \theta \le 1$. The superscript $^{n+\theta}$ denotes a time between t_n and t_{n+1} at which the mean value of flux is attained, see below. With this notation, (3.4.92) takes the form

$$E_i^{n+1} = E_i^n + \frac{\Delta t_n}{\Delta x} \left[Q_{i-1/2}^{n+\theta} - Q_{i+1/2}^{n+\theta} \right], \quad i = 1, ..., M, \ \ n = 0, 1, ... \tag{3.4.95}$$

Note than no approximations have been made so far, this is still *exact discrete conservation* of energy. It will update E_i to new time t_{n+1} once we specify how to compute the discrete fluxes. Also note that the updating scheme involves only the fluxes across the left and right faces of each control volume.

The first approximation comes from choosing a mean time for flux. For any $0 \leq \theta \leq 1$, we interpret the *mean time* $t_{n+\theta}$ as $t_{n+\theta} = (1-\theta)t_n + \theta t_{n+1}$, and assume that $Q^{n+\theta}_{i-1/2}$ is a convex combination of old $Q^n_{i-1/2}$ and new $Q^{n+1}_{i-1/2}$ values:

$$Q^{n+\theta}_{i-1/2} = (1-\theta)\, Q^n_{i-1/2} + \theta\, Q^{n+1}_{i-1/2}. \tag{3.4.96}$$

The standard choices for θ are 0, 1/2, 1:

- $\theta = 0$: Then the scheme is **explicit** (Forward Euler time-discretization). The right-hand side of (3.4.95) is known at t_n, so the update requires only evaluation. However, the time-step needs to be restricted to satisfy the Courant-Friedrichs-Lewy (CFL) stability condition, see (3.4.102),(3.4.103) below.
- $\theta = 1/2$: **Crank-Nicolson** scheme. It is implicit, so a system of equations needs to be solved at each time-step. It is unconditionally stable, but not positivity-preserving unless Δt is restricted, see (3.4.101) below.
- $\theta = 1$: **Backward Euler** scheme, it is implicit, so a system of equations needs to be solved at each time-step. It is unconditionally stable, and positivity-preserving, so the time-step needs to be restricted *only* for accuracy.

Discretization of (3.4.88): The second approximation comes from discretization of flux, which involves the gradient of temperature. Let T_i denote the mean temperature of control volume V_i, $i = 1, ..., M$, and T_0, T_{M+1} the temperatures at the end-points, consistently with our mesh. However, in order to approximate the gradient, the mean temperature T_i needs to be assigned to a specific location, which we take to be the node x_i of V_i. Then the natural discretization of Fourier's Law (3.4.88) for heat flux across face $x_{i-1/2}$, i.e. from x_{i-1} to x_i, is

$$Q_{i-1/2} = -k_{i-1/2}\, \frac{T_i - T_{i-1}}{x_i - x_{i-1}}, \quad i = 1, \ldots, M+1, \tag{3.4.97}$$

but we need to clarify the value of $k_{i-1/2}$. It represents an "effective" conductivity for heat transfer from node x_{i-1} to node x_i. But this involves two, possibly different, conductivities k_{i-1} and k_i. Instead, let us view Fourier's law in terms of **resistivity**= $R = \Delta x/k$, (which is additive, see [Alexiades and Solomon 1993, p.188], so we define

$$\text{Resistivity of the path } [x_{i-1}, x_i]: \quad R_{i-1/2} = \frac{x_{i-1/2} - x_{i-1}}{k_{i-1}} + \frac{x_i - x_{i-1/2}}{k_i}, \tag{3.4.98}$$

and write (3.4.97) as

$$Q_{i-1/2} = -\frac{T_i - T_{i-1}}{R_{i-1/2}}. \tag{3.4.99}$$

Apart from boundary conditions, which are discussed below, the above constitute a discretization for heat transfer (in 1-D), with or without phase change. Phase-change enters

via the EoS (3.4.85), in which case the nodal conductivities entering (3.4.98) can be taken to be

$$\frac{1}{k_i} = \frac{\lambda_i}{k_L} + \frac{1-\lambda_i}{k_S}, \tag{3.4.100}$$

with λ_i the liquid fraction of node $i = 1, \ldots, M$. For other options see [Alexiades and Solomon 1993, p.215].

Remark 4: Note that (3.4.97) is a centered finite difference approximation of the derivative, hence 2nd order, provided the face $x_{i-1/2}$ is chosen half-way between the nodes x_{i-1} and x_i, as is the case for a uniform mesh. Then the explicit and the fully implicit schemes are of 2nd order in space and 1st order in time, whereas Crank-Nicolson is 2nd order in both space and time.

Remark 5: It is possible to substitute E_i and fluxes in terms of temperature into (3.4.95) to obtain schemes for directly updating the temperature, with latent heat as a source term, [Shyy et al. 1996]. We do not recommend such formulations, see Remark 6.

The **Positive Coefficient Rule** is a simple and effective way to guarantee (strong) stability: when T_i^{n+1} is written as a linear combination of its neighbors T_{i-1}^n, T_i^n, T_{i+1}^n, all coefficients should be positive, [Patankar 1980]. This yields a restriction on the time-step and ensures the scheme will be **positivity-preserving** (non-negative values at t_n implies non-negative values at t_{n+1}), and thus free of unphysical oscillations. Positivity-preserving is stronger than and implies numerical stability. Applying the rule to the θ-scheme (3.4.95),(3.4.96),(3.4.99),(3.4.98), in the general case of non-uniform mesh and possibly variable properties (temperature-dependent and/or phase-dependent), the rule yields the

$$\textbf{strong CFL condition:} \qquad \mu \le \frac{1}{2(1-\theta)}, \qquad \text{with} \quad \mu = \frac{\Delta t_n}{\rho\, c_{pi}\, \Delta x_i}\, \frac{1}{R_{i\pm 1/2}}. \tag{3.4.101}$$

This shows that only the fully implicit scheme ($\theta = 1$) is trully unconditionally stable and positivity-preserving. All others need a restriction on the time-step to preserve positivity. Even though implicit schemes ($0 < \theta < 1$) are stable in the von Neumann sense (errors remain bounded), they can produce unphysical oscillations for large time-steps. The Crank-Nicolson scheme ($\theta = 1/2$) needs $\mu \le 1$, and the explicit scheme ($\theta = 0$) needs $\mu \le 1/2$.

The **explicit scheme** ($\theta = 0$) is, by far, the simplest and easiest to implement, as it does not involve any system solving. Moreover, it is also far easier to parallelize for concurrent computation on multi-processors (via domain decomposition using MPI message passing), for demanding problems. The only price to be paid for this simplicity and convenience is that the time-step Δt must be restricted to satisfy the CFL condition (3.4.101), which amounts to

$$\Delta t_n \le \frac{\rho\, c_{p\,i}\, \Delta x_i}{\frac{1}{R_{i-1/2}} + \frac{1}{R_{i+1/2}}}, \quad \text{or simply} \quad \Delta t_n \le \frac{\Delta x_{min}^2}{2\,\alpha_{max}}, \tag{3.4.102}$$

with $\Delta x_{min} = \min \Delta x_i$ and $\alpha_{max} = \max \alpha_i$. For uniform mesh and constant thermophysical properties it simplifies to the standard

$$\textbf{CFL condition:} \quad \Delta t \le \frac{\Delta x^2}{2\,\alpha}, \qquad \text{with} \quad \alpha = \frac{k}{\rho c_p}. \tag{3.4.103}$$

Discretization of boundary conditions
The standard types of boundary conditions are Dirichlet, Neumann, and convective (Robin) type. We discuss each type at $x = a$ for illustration.

I. Imposed temperature (Dirichlet) boundary condition: $T(a,t) = T_a(t) =$**given**.
Here the boundary temperature $T_0^n = T_a(t_n)$ is specified, so by (3.4.99), the boundary flux at $x = a$ is:

$$Q_{1/2}^n = -\frac{T_1^n - T_0^n}{R_{1/2}}, \quad \text{with} \quad R_{1/2} = \frac{x_1 - x_0}{k_1}. \tag{3.4.104}$$

Note that for a uniform mesh $x_1 - x_0 = \Delta x/2$.

II. Imposed flux (Neumann) boundary condition: $Q(a,t) = q_a(t) =$**given**.
Here the boundary flux $Q_{1/2}^n = q_a(t_n)$ is specified, which is all the scheme needs to proceed. However, the boundary temperature will change and needs to be found. Solving (3.4.104) for T_0, gives

$$T_0^n = T_1^n + R_{1/2}\, Q_{1/2}^n. \tag{3.4.105}$$

This involves the nodal value T_1, which will be updated from (3.4.95).
A very important particular case is that of an *insulated boundary*: $q_a(t) = 0$, so then $T_0^n = T_1^n$.

III. Convective boundary condition: $Q(a,t) = h\,[T_{amb}(t) - T(a,t)]$,
with $T_{amb}(t)$ a given ambient temperature. Here neither T nor Q is specified at the boundary, only a relation between them (Newton's law of cooling). Its discretization is $Q_{1/2}^n = h\,[T_{amb}(t_n) - T_0^n]$, or, using (3.4.103), $-\frac{T_1^n - T_0^n}{R_{1/2}} = h\,[T_{amb}(t_n) - T_0^n]$. Solving for T_0^n gives

$$T_0^n = \frac{T_1^n + h\,R_{1/2}\,T_{amb}^n}{1 + h\,R_{1/2}}. \tag{3.4.106}$$

Substituting this into the expression for $Q_{1/2}^n$ yields

$$Q_{1/2}^n = -\frac{T_1^n - T_{amb}^n}{R_{1/2} + 1/h}. \tag{3.4.107}$$

Observe that $h \to \infty$ amounts to the imposed temperature case (3.4.104), as it should.

Algorithm for the explicit Finite Volume scheme
We present the complete finite volume enthalpy algorithm for the melting problem mentioned at the beginning of §3.4.3.4-D. For simplicity, we assume constant c_S, c_S, k_S, k_L, and uniform mesh.

- Read in data: M, a, b, t_{end}
- Set $\Delta x = (b-a)/M$, the time-step Δt from (3.4.103), and $N_{steps} = t_{end}/\Delta t$.
- Declare arrays $x(0{:}M{+}1)$, $T(0{:}M{+}1)$, $E(1{:}M)$, $\lambda(1{:}M)$, $R(1{:}M{+}1)$, $Q(1{:}M{+}1)$. Note that there is no reason to index time into the arrays.
- Set initial values: $T_i = T_{init}(x_i)$, $E_i = E(T_i)$ from (3.4.85), and λ_i from (3.4.86), $i = 1{:}M$.
- Time-stepping: for $n = 1, \ldots, N_{steps}$, do:

1. Set the boundary fluxes $Q_{1/2}$, Q_{M+1} from (3.4.104)-(3.4.107), and internal fluxes from (3.4.99) $i = 2, \ldots, M$.
2. Update energies E_i from (3.4.95) to new time t_{n+1}.
3. Update λ_i from (3.4.86), and $R_{i-1/2}$ from (3.4.98),(3.4.100) to time t_{n+1}.
4. Update T_i from (3.4.85), and the boundary temperatures from (3.4.106),(3.4.105) to time t_{n+1}.

Now all quantities have been updated to new time and can go to 1. for the next time-step.

For a pure material melting at T_m, the algorithm will generate only one mushy control volume, say volume $i = m$ at time t_n, and then the front location at that time can be computed, for plotting, by

$$X^n = x_{m-1/2} + \lambda_m \, \Delta x_m. \tag{3.4.108}$$

Remark 6: The latent heat effect is only felt in mushy nodes, so each control volume should become mushy before changing phase. The above algorithm is robust in this respect, so skipping the transition indicates a bug or too large a time step. Some other implementations or algorithms may miss this, so one must be careful. Especially prone are schemes that directly update temperature either implicitly using too large a time-step, or they account for the latent heat via a source term.

Remark 7: The algorithm generarizes to 2 or 3 dimensions easily. Only need to define fluxes in the other directions, and the energy PDE will contain an additional pair of fluxes for each additional dimension. For example, in 2D Cartesian mesh of $M_x \times M_y$ nodes, there are two flux arrays: $Qx_{i-1/2,\,j}$ for $i = 1{:}M_x + 1$, $j = 1{:}M_y$ and $Qy_{i,\,j-1/2}$ for $i = 1{:}M_x$, $j = 1{:}M_y + 1$; the energy update (3.4.95) becomes:

$$E_{i,j}^{n+1} = E_i^n + \frac{\Delta t_n}{\Delta x \Delta y} \left[Q_{i-1/2,\,j}^n - Q_{i+1/2,\,j}^n + Q_{i,\,j-1/2}^n - Q_{i,\,j+1/2}^n \right], \quad i = 1{:}M_x,\ j = 1{:}M_y. \tag{3.4.109}$$

3.4.3.4-E Heat Capacity Method

The Heat Capacity Method is a fixed-domain, no-front tracking, temperature-based method that incorporates the latent heat into the heat capacity $c_p(T)$. Temperature is updated directly by the heat equation. It assumes non-isothermal phase change over some interval $[T_m - \Delta T, T_m + \Delta T]$, within which thermal properties are taken to be convex combinations of solid and liquid properties, interpolated by the liquid fraction λ. There are two main approaches: (i) Apparent Heat Capacity and (ii) Effective Heat Capacity.

(i) **Apparent Heat Capacity Method** was introduced by [Hashemi and Sliepcevich 1967] and has been developed by [Idelsohn et al. 1994], [Hu and Argyropoulos 1996], [Voller 1997]. This method is relatively popular today because it updates temperature directly from the heat equation, and can use experimental results to formulate an empirical expression for heat capacity. Dynamic measurements can be performed for pure and homogenous materials, utilizing Differential Scanning Calorimetry (DSC) with a Step Testing Method, [Castellon et al. 2008], [Gŭnther et al. 2009]. For example, [Fang and Medina 2009] used DSC to develop a mathematical formula for heat capacity of paraffinic products. In cases of non-uniform

materials and composite blends T-history method, [Zhang et al. 1999], or Dynamic Heat Flow Meter Apparatus measurements need to be applied, [Kosny et al. 2009 a,b], [Shukla et al. 2013]. Apparent heat capacity can be also estimated using numerical methods, [Lemmon 1981], [Voller 1997].

(ii) **Effective Heat Capacity Method** became known thanks to publications of [Heim and Clark 2004], [Minkowycz et al. 2006], [Muhieddine et al. 2009], [Poirier 1988]. Since the relationship between heat capacity and temperature is highly non-linear, an explicit scheme is often used. This may cause some inaccuracies in situation of sharp heat capacity changes with respect to temperature [Sadasivam et al. 2011]. For single-component cases with well-defined melting point T_m, the temperature range $2\Delta T$ should be as small as possible.

3.4.3.4-F Hybrid Methods

There is a large number of modified methods using components from one or both methods described above. We mention a couple such methods below.

Quasi-Enthalpy Method: [Pham 1985, 2006] introduced a hybrid scheme that consists of: (i) a temperature prediction step, and (ii) a verification and correction step in which the predicted temperatures are checked for consistency against the enthalpy-temperature curve and corrected if necessary. This method was introduced as one of the alternative numerical algorithms allowing phase change simulation in ESP-r, a whole building energy simulation program, [Sadasivam et al. 2011].

Improved Temperature-Based Equivalent Heat Capacity Method: [Cao and Faghri 1990], [Zhanhua and Yuwen 2006]. After a series of enhancements, this numerical model has been used in a number of projects, [Zeng and Faghri 1994a, 1994b], [Zhanhua and Yuwen 2006]. Today, this method is not in common use; however it offers an alternative to the Apparent Heat Capacity Method.

In large containers, natural convection in the liquid phase may impact overall system effectiveness. A study by [Ahmad et al. 2006] demonstrated that complexity of thermal model does not always yield improvements in simulation accuracy. In this work, numerical predictions generated by a complex thermal model considering a solid-liquid interface and results of a simpler model using the Effective Heat Capacity Method were compared. Recorded results showed that a simpler heat capacity approach was more accurate. In another similar study, finite element computer simulations were performed to compare accuracies of the Enthalpy and Heat Capacity Methods, [Lamberg et al. 2004]. When compared to experimental data, better agreement was obtained with the Heat Capacity Method.

A list of numerical methods used in the most popular whole-building energy simulation tools, with capability of modeling phase changes, is given in Table 3.4.2.

Table 3.4.2: Numerical methods used in best-known numerical tools which can be used for phase change simulations in buildings.

Whole-building computer tool	**Numerical method**	**Discretization**	**Time-stepping**	**References**
ESP-r	Effective heat capacity	Finite volume	Explicit	Heim,Clarke 2004
TRNSYS type 204, plus type 56	Effective heat capacity	Finite element	Crank-Nicolson	Jokisalo et al. 2000
TRNSYS type 222, plus type 56	Indirect calculatns			Ibanez et al. 2005
TRNSYS type 241, plus type 56	Enthalpy method	Finite difference		Schranzhofer et al. 2006
TRNSYS type 260, plus type 56	Effective heat capacity	Finite difference	Explicit	Kuznik et al. 2010
TRNSYS type 399, plus type 56	Two different methods available based on the heat capacity approach	Finite element	Crank-Nicolson	Dentel, Stephan 2013
MATLAB	Enthalpy method	Finite volume	Crank-Nicolson	Sadasivam et al. 2011
EnergyPlus	Enthalpy method	Finite difference	Implicit	Pedersen 2007

References

Ahmad M., Bontemps A., Salle H., Quenard D. (2006) Thermal Testing and Numerical Simulation of a Prototype Cell Using Light Wallboards Coupling Vacuum Insulation Panels and Phase Change Materials. *Energy and Buildings* 38: 673681.

Albert M.R. and ONeill K. (1986) Moving Boundary-Moving Mesh Analysis of Phase Change Using Finite Elements with Transfinite Mappings. *Intl. J. Numerical Methods in Engineering* 23(4): 591607.

Alexiades V., Solomon A.D. (1993) *Mathematical Modeling of Melting and Freezing Processes*. Hemisphere Publ. Corp.

Alexiades V., Autrique D. (2010) Enthalpy Model for Heating, Melting and Vaporization in Laser Ablation. *Electronic J. Differential Equations*, Conf.19: 114.

AL-Saadi S.N. and Zhai Z. (2013) Modeling Phase Change Materials Embedded in Building Enclosure: A Review. *Renewable and Sustainable Energy Reviews* 21: 659673.

Basu B. and Date A. (1988) Numerical Modeling of Melting and Solidification Problems - a Review. *Sadhana Academy Proceedings in Engineering Sciences* 13: 169213.

Bonnerot R. and Janet P. (1977) Numerical Computation of the Free Boundary for the Two-Dimensional Stefan Problem by Space–Time Finite Elements. *J. Computational Physics* 25: 163-181.

Cao Y. and Faghri A.A. (1990) Numerical Analysis of Phase-Change Problems Including

Natural Convection. *J. Heat Transfer* 112: 812816.

Carslaw H.S. and Jaeger J.C. (1959) *Conduction of Heat in Solids.* Clarendon Press, Oxford.

Castellon C, Gŭnther E, Mehling H, Hiebler S, Cabeza L.F. (2008) Determination of the Enthalpy of PCM as a Function of Temperature Using a Heat-Flux DSC-A Study of Different Measurement Procedures and Their Accuracy, *Intl. J. Energy Research* 32(13): 12581265.

Chuang Y.K. and Szekely J. (1972) On the Use of Greens Functions for Solving Melting and solidification problems. *Intl. J. Heat Mass Transfer* 15: 1171-1174.

Colin J. (2014) Morphological Instability of a Stressed Solid Cylinder in the Solidification and Melting Regimes. *J. Crystal Growth* 402: 113118.

Crank J. (1981) How to Deal with Moving Boundaries", pp. 177-200 in *Thermal Problems. Numerical Methods in Heat Transfer*, Edited by R.W. Lewis, K. Morgan, O.C. Zienkiewicz, Wiley, New York.

Crank J. (1984) *Free and Moving Boundary Problems.* Clarendon Press, Oxford.

Crank J. and Gupta R. (1975) - Isotherm Migration Method in Two Dimensions. *Intl. J. Heat Mass Transfer* 18: 1101-1117.

Dentel A. and Stephan W. (2013) TRNSYS TYPE 399, Phase Change Materials in Passive and Active Wall Constructions; Model Description and Implementing into TRNSYS. Georg Simon Ohm University of Applied Sciences, Institute for Energy and Building. Version 1.5, May 2013, Germany - http://www.transsolar.com/_software/download/de/ts_type_399_en.pdf

Douglas J. and Gallie T.M. (1955) On the Numerical Integration of a Parabolic Differential Equation Subject to a Moving Boundary Condition, *Duke Math. J.* 22: 557571.

Dusinberre G.M. (1945) Numerical Methods for Transient Heat Flow. *Transactions ASME* 67: 703712.

Dutil Y., Rousse D.R., Salahb N.B., Lassue S., Zalewski S. (2011) A Review on Phase-Change Materials: Mathematical Modeling and Simulations. *Renewable and Sustainable Energy Reviews* 15(1): 112130.

Evans G.W. (1951) A note on the Existence of a Solution to a Problem of Stefan. *Quarterly Appl. Math.* 9: 185193.

Eyres N.R., Hartree D.R., Ingham J., Jackson R., Sarjant R.J. and Wagstaff S.M. (1946) - The Calculation of Variable Heat Flow in Solids, *Phil. Trans. R. Soc. A* 240: 1-57.

Fang Y. and Medina M. (2009) Proposed Modifications for Models of Heat Transfer Problems Involving Partially Melted Phase Change Processes. *J. ASTM International* 6(9) ISSN: 1546-962X.

Farid M.M., Khudhair A.M., Razack S.A.K., Al-Hallaj S. (2004) A Review on Phase Change Energy Storage: Materials and Applications." *Energy Convers. Manage.* 45(9-10): 1597-1615.

Fox, L. (1975) What are the Best Numerical Methods?", pp. 210-241 in *Moving Boundary Problems in Heat Flow and Diffusion.* Edited by J.R. Ockendon and W.R. Hodgkins. Clarendon Press, Oxford.

Glimm J., Grove J.W., Li X.L., Shyue K.-M., Zhang Q., and Zeng Y. (1998) Three Dimensional Front Tracking. *SIAM J. Sci. Comp.* 19: 703727.

Gŭnther E., Hiebler S., Mehling H., Redlich R. (2009) Enthalpy of Phase Change Materials as a Function of Temperature: Required Accuracy and Suitable Measurement Methods. *Intl J. Thermophysics* 30: 12571269.

Hashemi H.T. and Sliepcevich C.M. (1967) A Numerical Method for Solving Two-Dimensional Problems of Heat Conduction with Change of Phase. *Chemical Engineering Prog Symp series* 63: 3441.

Heim D. and Clarke J.A. (2004) Numerical Modeling and Thermal Simulation of PCMGypsum Composites with ESP-r. *Energy and Buildings* 36: 795805.

Hill J.M. (1987) *One-Dimensional Stefan Problems: An Introduction.* Longman Scientific Technical, Harlow.

Hong C.P., Umeda T. and Kimura Y. (1984) Numerical Models for Casting Solidification: Part II. Application of the boundary element method to solidification problems. *Metallurgical Transactions B*, 15(1): 101-107.

Hsiao J.S. (1985) An Efficient Algorithm for Finite-Difference Analysis of Heat Transfer with Melting and Solidification. *Numer. Heat Transfer* 8: 653-666.

Hu H. and Argyropoulos S.A. (1996) Mathematical Modelling of Solidification and Melting: A Review. *Modelling and Simulation in Materials Science and Engineering* 4: 371396.

Ibanez M., Lazaro A., Zalba B., Cabeza L.F. (2005) An Approach to the Simulation of PCMs in Building Applications using TRNSYS. *Appl. Therm. Eng.* 25: 17961807.

Idelsohn S., Storti M., Crivelli L. (1994) Numerical Methods in Phase-Change Problems. *Archives Computat. Methods in Eng.* 1: 4974.

Javierre E., Vuik C., Vermolen F.J. and van der Zwaag S. (2006) - A comparison of numerical models for one-dimensional Stefan problems, *J. Computat. & Applied Math.* 192: 445–459.

Jokisalo J., Lamberg P., Siren K. (2000) Thermal Simulation of PCM Structures with TRNSYS. *Proceedings of the 8 th International Conference on Thermal Energy Storage.* Stuttgart, Germany 2000.

Kim K.M. (1978) Morphological Instability under Constitutional Supercooling during the Crystal Growth of InSb from the Melt under Stabilizing Thermal Gradient , *J. Crystal Growth* 44(4): 403-413.

Kośny J., Stovall T. K., Yarbrough D.W. (2009a) - Dynamic Heat Flow Measurements to Study the Distribution of Phase-Change Material in an Insulation Matrix. *Proceedings of the 2009 International Thermal Conductivity Conference (ITCC) and the International Thermal Expansion Symposium (ITES)*, Aug.29-Sep.2, 2009 Pittsburgh, PA USA.

Kośny J., Kossecka E., Yarbrough D.W. (2009b) Use of a Heat Flow Meter to Determine Active PCM Content in an Insulation. *Proceedings of the 2009 International Thermal Conductivity Conference (ITCC) and the International Thermal Expansion Symposium (ITES)*, Aug.29-Sep.2, 2009 Pittsburgh, PA USA.

Kuznik F., Virgone J., Johannes K. (2010) - "Development and Validation of a New TRNSYS Type for the Simulation of External Building Walls Containing PCM." *Energy and Buildings* 42 (7): 1004-1009.

Lamberg P., Lehtiniemi R., Henell A.M. (2004) Numerical and Experimental Investigation of Melting and Freezing Processes in Phase Change Material Storage. *Intl. J. Thermal Sciences* 43: 277-287.

Lazaridis A. (1969) A Numerical Solution of the Solidification (or Melting) Problem in Multidimensional Space. PhD dissertation, Columbia University.

Lemmon E. (1981) Multidimensional Integral Phase Change Approximations for Finite Element Conduction Codes., pp. 201213 in *Numerical Methods in Heat Transfer*, editors R.W. Lewis, K. Morgan, O.C. Zienkiewicz. New York: Wiley.

Lupis C.H.P. (1983) *Chemical Thermodynamics of Materials.* Prentice Hall, Englewood Cliffs, New Jersey.

Lynch R.D. (1982) Unified Approach to Simulation on Deforming Elements with Application to Phase Change Problems. *J. Computational Physics* 47(3): 387-411.

Mehling H. and Cabeza L.F. (2008) *Heat and cold storage with PCM.* Sprinegr.

Minkowycz W.J., Sparrow E.M., Murthy J.Y. Editors, (2006) *Handbook of Numerical Heat Transfer.* 2nd edition, Wiley, 2006.

Muhieddine M., Canot E., March R. (2009) Various Approaches for Solving Problems in Heat Conduction with Phase Change. *Intl. J. Finite Volumes* 6(1): 120.

Murray W.D. and Landis F. (1959) - Numerical and Machine Solutions of the Transient Heat Conduction Problems Involving Melting or Freezing. *J. Heat Transfer* 81: 106-112.

ONeill K. (1983) Boundary Integral Equation Solution of Moving Boundary Phase Change Problems. *Intl. J. Numer. Meth. Eng.* 19: 18251850.

Osher S.J. and Fedkiw, R.P. (2002). *Level Set Methods and Dynamic of Implicit Surfaces.* Springer-Verlag.

Ozisik M.N. (1993) *Heat Conduction*, 2nd ed. Wiley.

Patankar S.V. (1980) *Numerical Heat Transfer and Fluid Flow*, Hemisphere.

Pedersen C.O. (2007) Advanced Zone Simulation in EnergyPlus: Incorporation of Variable Properties and Phase Change Materials (PCM) Capability, pp.1341-1345 in *Proceedings of the 10th International IBPSA Conference.* Beijing, China.

Pham Q.T. (1985) A Fast, Unconditionally Stable Finite-Difference Scheme for Heat Con-

duction with Phase Change. *Intl. J. Heat and Mass Transfer* 28: 20792084.

Pham Q.T. (2006) Modeling Heat and Mass Transfer in Frozen Foods: A Review. *Intl. J. Refrigeration* 29: 876888.

Poirier D.J. (1988) On Numerical Methods Used in Mathematical Modeling of Phase Change in Liquid Metals. *J. Heat Transfer* 110: 562570.

Qin R.S. and Bhadeshia H.K. (2010) - "Phase field method" Review, *Materials Science and Technology* 26(7): 803-811.

Ralph W. and Bathe K.-J. (1982) An Efficient Algorithm for Analysis of Nonlinear Heat Transfer with Phase Changes. *Intl. J. Numer. Meth. Eng.* 18: 119-134.

Rao P. and Sastri V.M.K. (1984) "Efficient Numerical Method for Two-Dimensional Phase Change Problems. *Intl. J. Heat Muss Transfer* 27: 2077-2084.

Roose J., Storrer W.0. (1984) Modeling of Phase Changes by Fictitious Heat Flow. *Intl. J. Numer. Meth. Eng.* 20: 217-225.

Rubinstein L.I. (1971) *The Stefan Problem.* Amer. Math. Soc. (Translated from 1967 Russian edition).

Sadasivam S., Almeida F., Zhang D., Fung A.S. (2011) Aniterative Enthalpy Method to Overcome the Limitations in ESP-rs PCM solution algorithm. *ASHRAE Transactions* 117: 100107.

Schranzhofer H., Puschnig P., Heinz A., Streicher W. (2006) Validation of a TRNSYS Simulation Model for PCM Energy Storages and PCM Wall Construction Elements. *Proceedings of ECOSTOCK 2006 10th International Conference on Thermal Energy Storage* Pomona, NJ, USA.

Sethian James A. (1999). *Level Set Methods and Fast Marching Methods : Evolving Interfaces in Computational Geometry, Fluid Mechanics, Computer Vision, and Materials Science.* Cambridge University Press.

Shukla N., Cao P., Kośny J. (2013) Lab-scale Dynamic Thermal Testing of PCM-enhanced Building Materials. *Proceedings of the ASTM Symposium on Next-Generation Thermal Insulation Challenges and Opportunities*, October 23-24, 2013, Jacksonville, FL, USA.

Shyy W., Vdaykumar H.S., Rae M.M., Smith R.W. (1996) *Computational Fluid Dynamics with Moving Boundaries.* Hemisphere, Washington, DC.

Sun Y. and Beckermann C. (2007) - "Sharp interface tracking using the phase-field equation", *J. Computational Physics* 210: 626-653.

Uverdi S.O. and Tryggvason G. (1992) - A Front Tracking Method for Viscous, Incompressible Multi-Fluid Flows, *J. Computational Physics* 100: 25-37.

Voller V.R. (1997) An Overview of Numerical Methods for Solving phase Change Problems. pp. 341380 in *Advances in Numerical Heat Transfer*, editors Minkowycz W.J., Sparrow E.M., Taylor&Francis.

Voller V.R., Swenson J.B., Kim W., Paola C. (2006) -An Enthalpy Method for Moving Boundary Problems on the Earths Surface. *Intl. J. Numerical Methods for Heat and Fluid Flow* 16(6): 4154.

Zabaras N. and Ruan Y. (1990) - Moving and Deforming Finite Element Simulation of Two-Dimensional Stefan Problems. *Commun. Applied Numer. Meth.* 6(7): 495-506.

Zaeema M.A. and Mesarovicb S.D. (2011) Morphological Instabilities in Thin Films: Evolution Maps. *Computational Materials Science* 50(3): 10301036.

Zeng X., Faghri A. (1994a) Temperature-Transforming Model for Binary Solid-Liquid Phase–Change Problems. Part I: Mathematical Modeling and Numerical Methodology. *Numerical Heat Transfer B* 25: 467480.

Zeng X., Faghri A. (1994b) Temperature-Transforming Model for Binary Solid-Liquid Phase–Change Problems. Part II: Numerical Simulation. *Numerical Heat Transfer B* 25: 481500.

Zhang Y., Jiang Y. and Jiang Y. (1999) A Simple Method, the T-History Method, of Determining the Heat of Fusion, Specific Heat and Thermal Conductivity of Phase-Change Materials. *Measurement Science and Technology* 10: 201205.

Zhanhua M. and Yuwen Z. (2006) Solid Velocity Correction Schemes for a Temperature Transforming Model for Convection Phase Change. *Intl. J. Numerical Methods for Heat and Fluid Flow* 16: 204225.